Generating Superbasic Sites on Mesoporous Silica SBA-15

Zheng Ying Wu, Qi Jiang, Yi Meng Wang, Hong Ji Wang, Lin Bing Sun, Li Ying Shi, Jia Hui Xu, Ying Wang, Yuan Chun, and Jian Hua Zhu*

School of Chemistry and Chemical Engineering, Nanjing University, Nanjing 210093, China

Received April 7, 2006. Revised Manuscript Received June 12, 2006

Superbasic sites have been generated on the mesoporous silica materials for the first time, through a new strategy to prepare the MgO-modified SBA-15 in one-pot synthesis and then to disperse KNO_3, possessing the good textural structure of the host and the high basic strength (H_-) of 27.0. The in situ coated Mg species passivated the silanol groups on the surface of siliceous SBA-15 so that the mesostructure of SBA-15 could be reserved after the composite was loaded with KNO_3 and activated at high temperature. Existence of the special protection layer of MgO on the surface of SBA-15 was also beneficial for decomposition of KNO_3 to form superbasic sites on the mesoporous silica. The influence of coating amount of MgO on the protection of the textural properties of SBA-15 is examined and discussed in terms of consuming surface silanol groups. Dispersion and decomposition of KNO_3 on the MgO layer is also explored. Other metal oxides such as CaO, ZnO, and Al_2O_3 are in situ coated on the surface of SBA-15 through one-pot synthesis and their function of protecting SBA-15 is evaluated for comparison with MgO.

Introduction

Adsorption and catalysis by solid strong bases have a considerable potential for many important chemical processes in industry,[1] especially for the basic selective reactions to produce fine chemicals.[2,3] Apart from mercaptane oxidation in petroleum refining, formation of carbon−carbon bond in fine chemistry and (trans-) esterification in pharmaceutical and cosmetic industries,[4] one of the noteworthy base-catalyzed reactions is the preparation of 4-methylthiazole. The conventional industrial route to 4-methylthiazole is a multistep process using several hazardous chemicals, while it can be directly synthesized from SO_2 and imine over a basic zeolite by a new environmentally benign method. Among the solid bases, basic zeolites are widely used as shape-selective catalysts in their ion-exchanged or impregnated forms, and the former exhibit relatively weak basicity while the latter have strong basic sites.[5−7] Ono and co-workers developed a new preparative method to enhance the potential of basic zeolites,[8] and the resulting rare-earth elements modified alkali-exchanged zeolite Y samples could display the catalytic properties as a superbase. Through the dispersion of KNO_3 on zeolite KL, another superbasic material was also obtained.[9,10] Nowadays, solid superbases are highly desired for green chemistry and many efforts have been made for synthesis and application of new solid superbases.[11−16] Regardless of the great amount of work dedicated to basic zeolites and related crystalline molecular sieves, the dimension and accessibility of pores were restrained to the sub-nanometer scale. The small pore opening of zeolites prevents bulky molecules from reaching the active sites, which limited application of basic zeolites.[7] On the other hand, mesotextured materials with long-range ordered topological structures always have larger surface areas and pore volumes than zeolites.[17] So synthesis of solid mesoporous base or using mesoporous materials as carriers for generating basic species is requested. Nevertheless, it is difficult to prepare mesoporous materials with superbasicity. Ordered mesoporous MgO with high thermal stability has even been synthesized by exotemplating using CMK-3 carbon, and its basicity is comparable to the MgO-coated SBA-15 samples.[18] However, this "hard"-templating route is not easy to replicate so many methods are developed based on doping of the host materials with basic guest species.

* To whom correspondence should be addressed. E-mail: jhzhu@netra.nju.edu.cn. Fax: +86-25-83317761. Tel: +86-25-83595848.

(1) Ono, Y.; Baba, T. *Catal. Today* **1997**, *38*, 321.
(2) Baba, T.; Kizuka, H.; Handa, H.; Ono, Y. *Appl. Catal., A* **2000**, *194*, 203.
(3) Baba, T.; Kato, A.; Yuasa, H.; Toriyama, F.; Handa, H.; Ono, Y. *Catal. Today* **1998**, *44*, 271.
(4) Weitkamp, J.; Hunger, M.; Rymsa, U. *Microporous Mesoporous Mater.* **2001**, *48*, 255.
(5) Kirschhock, C. E. A.; Hunger, B.; Martens, J.; Jacobs, P. A. *J. Phys. Chem. B* **2000**, *104*, 439.
(6) Brilhac, J.-F.; Sultana, A.; Gilot, P.; Martens, J. A. *Environ. Sci. Technol.* **2002**, *36*, 1136.
(7) Hattori, H. *Chem. Rev.* **1995**, *95*, 537.
(8) Yoshida, T.; Tanaka, T.; Yoshida, S.; Hikita, S.; Baba, T.; Ono, Y. *Solid State Commun.* **2000**, *114*, 255.
(9) Zhu, J. H.; Chun, Y.; Wang, Y.; Xu, Q. H. *Catal. Today* **1999**, *51*, 103.
(10) Zhu, J. H.; Chun, Y.; Wang, Y.; Xu, Q. H. *Mater. Lett.* **1997**, *33*, 207.
(11) Arumugam, S.; Verkade, J. G. *J. Org. Chem.* **1997**, *62*, 4827.
(12) Matsuhashi, H.; Klabunde, K. J. *Langmuir* **1997**, *13*, 2600.
(13) Matsuhashi, H.; Oikawa, M.; Arata, K. *Langmuir* **2000**, *16*, 8201.
(14) Suzukamo, G.; Fukao, M.; Hibi, T.; Tanaka, K.; Minobe, M. *Stud. Surf. Sci. Catal.* **1997**, *108*, 649.
(15) Gorzawski, H.; Hoelderich, W. F. *J. Mol. Catal. A-Chem.* **1999**, *144*, 181.
(16) Li, Z. J.; Prescott, H. A.; Deutsch, J.; Trunschke, A.; Liske, H.; Kemnitz, E. *Catal. Lett.* **2004**, *92*, 175.
(17) Soler-Illia, G. J. A. A.; Sanchez, C.; Lebeau, B.; Patarin, J. *Chem. Rev.* **2002**, *102*, 4093.
(18) Roggenbuck, J.; Tiemann, M. *J. Am. Chem. Soc.* **2005**, *127*, 1096.

10.1021/cm0608138 CCC: $33.50
Published on Web 08/23/2006

Among the candidates with mesostructure, mesoporous silicas seem to be the cheapest, and introducing basic guests or their precursors such as cesium acetate into the mesoporous host such as MCM-41 is a feasible way for preparing a superbase.[9] However, the cesium-modified material did not show good thermal and chemical stability because the cesium oxides could corrode and damage the siliceous framework of the host at high temperature.[19] Organic bases grafted mesoporous materials such as aminopropyl-modified HMS[20] and aminopropyl-functionalized SBA-15[21] were prepared by using silanizing agents, but these organic−inorganic composites need to be used in mild conditions below high temperature. Thermal treatment of mesoporous materials such as the M41S family with ammonia to prepare nitrogen-incorporated silicon oxynitride at high temperature provided an interesting way for obtaining mesoporous base.[22,23] Wang and Liu[24] subsequently revealed that the treating temperature controlled the nitrogen content of the oxynitride materials but the basicity of such materials needs to be improved further. Loading KNH_2 on porous silicon nitride can produce superbasicity,[25] but the rigorous synthetic conditions and the oxygen sensitivity hinder its application. Thus, searching for new ways to prepare solid mesoporous superbase becomes a challenge in the study of basic materials. Dispersion of neutral potassium salt like KNO_3 on a porous host followed by thermal treatment can create superbasic sites on Al_2O_3[26] and ZrO_2.[27] Apart from their low cost and the convenience in preparation, KNO_3-modified superbasic materials possess the advantage in storage because they do not exhibit superbasicity until activation at high temperature, which is beneficial for their potential application in industry. However, loading KNO_3 onto zeolites could not form superbasic sites,[28] with only one exception of KL,[10] because the silicon content in the framework of zeolite preferentially reacted with the potassium to form the basic species with low strength.[29] Likewise, it is hopeless to obtain superbasicity on mesoporous silica if KNO_3 is directly dispersed on the porous hosts.

In this paper, we try a new strategy to generate superbasic sites on mesoporous silica via a MgO interlayer that exists between silicon skeleton and potassium species. A special mesoporous support with a layer of wrapped MgO is prepared by a one-pot method,[30] and then the neutral potassium salt KNO_3 is loaded on the MgO-coated SBA-15, followed by thermal activation to convert the precursor to potassium oxide nanoparticles. As a result, the mesoporous structure of SBA-15 can be retained with a comparatively large surface area, which is beneficial for potential application in adsorption, separation, and catalysis. At the same time, an unusual strong basicity appears on the mesoporous composite. This paper aims to explore the special function of the MgO layer in protecting the mesostructure of SBA-15 and to discuss whether the precoated MgO has the ability to promote dispersion and/or decomposition of potassium and then formation of basic sites. Some other metal oxides, besides MgO, are also employed to protect the SBA-15, to further comprehend the function of MgO in the formation of superbasic sites.

Experimental Section

Preparation of SBA-15 was adapted from the published procedure by Zhao et al.[31] The MgO in situ coated mesoporous silica was prepared as follows: 2 g of triblock copolymer P123 ($EO_{20}PO_{70}EO_{20}$, Aldrich) and a calculated amount of magnesium acetate were dissolved in 75 g of 1.6 M HCl, and then 4.25 g of tetraethyl orthosilicate (TEOS) was added under stirring at 313 K. The molar composition of the mixture was 1:0.02:*X*:6:192 TEOS:P123:Mg$(CH_3COO)_2$:HCl:H_2O, where *X* varied from 0.02 to 0.64, corresponding to the mass percentages of MgO that precoated on SBA-15 from 1% to 30%, respectively. The solution was stirred for 24 h at 313 K and heated at 373 K for another 24 h under static conditions. Finally, the liquid was evaporated with stirring at 353 K, instead of being filtered off in the traditional synthesis of SBA-15. The solid obtained was dried at 353 K and calcined at 823 K for 6 h to remove template and to form MgO at the same time. The resulting MgO/SBA-15 samples are denoted as MS(*y*) where *y* represents the mass percentages of MgO. Other oxide-modified SBA-15 samples were synthesized under the otherwise same conditions as MS(*y*) with the calculated amount of different precursors.

The potassium salt multicoated sample was prepared with a procedure similar to that reported previously,[26,32] grinding KNO_3 and MS(*y*) at a different weight ratio with a small amount of water, followed by drying at 373 K. The final samples are denoted as *x*KMS(*y*), where *x* and *y* represent the mass percentage of the KNO_3 and MgO in the composites, respectively. And the sample of *x*KS is the bare SBA-15 loaded with KNO_3. After the multicoated samples were activated at 873 K in a N_2 flow, their structures were detected by XRD, TEM, and N_2 adsorption−desorption methods. The XRD patterns were recorded on an ARL XTRA diffractometer with Cu Kα radiation in the 2θ range from 0.8 to 8° or from 5 to 80°. TEM and EDX analysis was performed on a FEI Tecnai G^2 20 S-TWIN electron microscope operating at 200 kV.

The N_2 adsorption and desorption isotherms at 77 K were measured using a Micromeritics ASAP 2000 system. The samples were outgassed at 573 K for 4 h prior to testing. The Brunauer−Emmett−Teller (BET) specific surface area was calculated using adsorption data in the relative pressure range from 0.04 to 0.2. The total pore volume was determined from the amount adsorbed at a relative pressure of about 0.99. The pore size distribution curves were calculated from the analysis of the adsorption branch of the

(19) Kloetstra, K. R.; van Bekkum, H. *Stud. Surf. Sci. Catal.* **1997**, *105*, 431.
(20) Macquarrie, D. J.; Jackson, D. B.; Tailland, S.; Utting, K. A. *J. Mater. Chem.* **2001**, *11*, 1843.
(21) (a) Wang, X. G.; Lin, K. S. K.; Chan, J. C. C.; Cheng, S. *Chem. Commun.* **2004**, 2762. (b) Wang, X.; Lin, K. S. K.; Chan, J. C. C.; Cheng, S. *J. Phys. Chem. B* **2005**, *109*, 1763.
(22) Haskouri, J. E.; Cabrera, S.; Sapina, F.; Latorre, J.; Guillem, C.; Beltran-Porter, A.; Beltran-Porter, D.; Marcos, M. D.; Amoros, P. *Adv. Mater.* **2001**, *13*, 192.
(23) Xia, Y.; Mokaya, R. *Angew. Chem., Int. Ed.* **2003**, *42*, 2639.
(24) Wang, J. C.; Liu, Q. *Microporous Mesoporous Mater.* **2005**, *83*, 225.
(25) Kaskel, S.; Schlichte, K. *J. Catal.* **2001**, *201*, 270.
(26) Yamaguchi, T.; Zhu, J. H.; Wang, Y.; Komatsu, M.; Ookawa, M. *Chem. Lett.* **1997**, *10*, 989.
(27) Wang, Y.; Huang, W. Y.; Wu, Z.; Chun, Y.; Zhu, J. H. *Mater. Lett.* **2000**, *46*, 198.
(28) Zhu, J. H.; Wang, Y.; Chun, Y.; Wang, X. S. *J. Chem. Soc., Faraday Trans.* **1998**, *94*, 1163.
(29) Zhu, J. H.; Chun, Y.; Qin, Y.; Xu, Q. H. *Microporous Mesoporous Mater.* **1998**, *24*, 19.
(30) Wei, Y. L.; Wang, Y. M.; Zhu, J. H.; Wu, Z. Y. *Adv. Mater.* **2003**, *15*, 1943.
(31) Zhao, D. Y.; Feng, J. L.; Huo, Q. S.; Melosh, N.; Fredrickson, G. H.; Chmelka, B. F.; Stucky, G. D. *Science* **1998**, *279*, 548.
(32) Wang, Y.; Huang, W. Y.; Chun, Y.; Zhu, J. H. *Chem. Mater.* **2001**, *13*, 670.

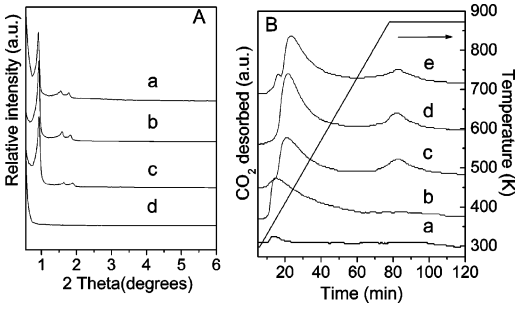

Figure 1. (A) Low-angle XRD patterns of (a) SBA-15, (b) MS(20), (c) 26KMS(20), and (d) 26KS samples. (B) CO_2-TPD spectra of (a) SBA-15, (b) MS(20), (c) 20KMS(20), (d) 26KMS(20), and (e) 35KMS(20) samples.

isotherm using the Barrett−Joyner−Halenda (BJH) algorithm. FT-IR experiments were performed on a set of BRUKER 22 FT-IR spectrometers. Raman spectra were obtained in Microscope-based Raman systems (Ranishaw in-vira). An argon ion laser operating at 514 nm supplied the excitation. All Raman scattering measurements were accomplished at room temperature. Potassium contents of the multicoated samples were measured by inductive coupled plasma-atomic emission spectrometry (ICP-AES).

In CO_2-TPD experiments, a 50 mg sample was heated in a flow of He (99.999%) at a rate of 8 K/min to 873 K and kept at 873 K for 2 h. Prior to adsorption of CO_2 (99.999%) at 298 K, blank TPD was carried out from 298 to 873 K to confirm no desorption occurred. After the physical adsorbed CO_2 was purged by a He flow at 298 K for 2 h, CO_2-TPD was performed up to 873 K at the rate of 8 K/min, and the CO_2 liberated was detected by an "on-line" Varian 3380 chromatograph with a thermal conductivity detector.[32] The basic strength of the samples was measured by use of a Hammett indicator as described previously,[29] while the soluble basicity was determined by conventional titration.[11] Temperature-programmed decomposition (TPDE) of the KS and KMS samples were carried out in a microreactor. A sample of 8−10 mg, in 20−40 mesh, was heated in a flow of N_2 (30 mL/min) from 293 to 873 K at a rate of 10 K/min. The gaseous products nitrogen oxides liberated in the process were converted to NO_2 by passing through a CrO_3 tube and then absorbed in a solution of sulfanilamide and *N*-1-naphthylethylenediamine di-HCl. The amount of NO_2 was detected by colorimetric method and represented the amount of KNO_3 decomposed.[33]

Results and Discussion

(A) Characterization of New Mesoporous Solid Strong Base. Figure 1 depicts the XRD patterns of the multicoated SBA-15 samples. The 26KMS(20) composite, consisting of 26 wt % KNO_3 dispersed on the SBA-15 host precoated with 20 wt % MgO, exhibits the typical X-ray diffraction patterns of the two-dimensional hexagonal pore ordering of the *p*6*mm* space group. As shown in Figure 1c, a well-resolved pattern with a prominent peak at 2θ of 0.9° accompanied by two weak peaks at 1.6° and 1.9°, indexed as (100), (110), and (200) reflections corresponding to *p*6*mm* hexagonal symmetry, matches well with the pattern of parent SBA-15 (Figure 1a). This XRD result indicates that the ordered mesostructure of the siliceous SBA-15 is preserved, even though the KNO_3 has been introduced and converted to the strong basic potassium species. The transmission electron

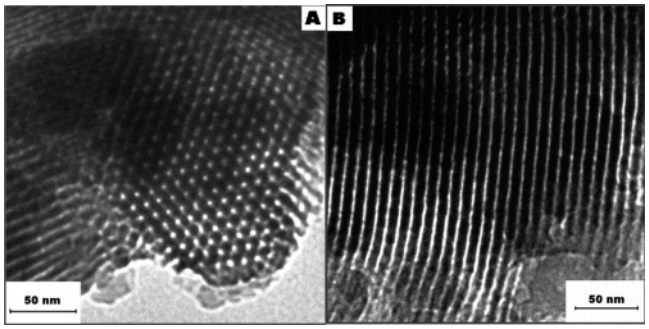

Figure 2. Transmission electron micrographs of 26KMS(20) sample.

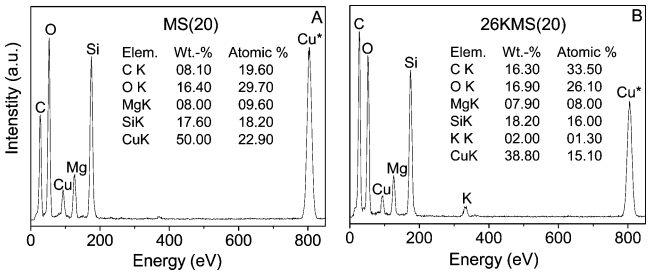

Figure 3. EDX spectra of (A) MS(20) and (B) 26KMS(20) samples. (Cu* means the Cu support grid).

microscopy (TEM) micrographs in Figure 2 provide further proof on the preservation of hexagonal mesostructure in the 26KMS(20) composite. In the micrographs taken with the beam direction parallel to the pore direction (Figure 2A), the hexagonally ordered pore structure can be distinguished but no potassium species particles are visualized. Likewise, there are only the images of channels and frameworks of the host on the micrographs taken with the beam direction perpendicular to the pores internal surfaces of SBA-15 (Figure 2B); the straight uniform channels and hexagonal pores are clearly visible and no guest particles on the outside surface of SBA-15 are observed either. The particles could not be found in the channels of SBA-15 by the TEM method, probably because of the weak contrast between the silica frameworks of SBA-15 and the oxide particles.[34] Further, the thickness of the mesoporous wall estimated from the TEM images (about 5.8 nm) is a bit larger than the value calculated from the nitrogen adsorption results (4.2 nm), probably due to the fact that the electron beam cannot completely irradiate in vertical orientation. Schuth et al.[35] has reported that the diameter of the white line in TEM does not necessarily correspond to the diameter of the mesopore. EDX analysis was performed to estimate the local composition of MS(20) and 26KMS(20) samples, in which the magnesium signal can be clearly observed in the former while both magnesium and potassium signals emerge in the latter (Figure 3). Although random areas were selected to detect the EDX results, the resultant Si/Mg and Si/K atomic ratios are similar, indicating a comparatively good distribution of the magnesium and potassium species inside the samples. Meanwhile, the Si/Mg ratio in MS(20) is close to that in 26KMS(20), which implied that introducing potassium

(33) Shen, B.; Chun, Y.; Zhu, J. H.; Wang, Y.; Wu, Z.; Xia, J. R.; Xu, Q. H. *Physchemcomm.* **1999**, *2*, 9.

(34) Zhang, W.-H.; Shi, J.-L.; Wang, L.-Z.; Yan, D.-S. *Chem. Mater.* **2000**, *12*, 1408.

(35) Janssen, A. H.; Yang, C.-M.; Wang, Y.; Schu1th, F.; Koster, A. J.; de Jong, K. P. *J. Phys. Chem. B* **2003**, *107*, 10552.

Scheme 1. Schematic Diagram of the Multicoating Procedure for Generating Superbasic Sites on Mesoporous Silica SBA-15

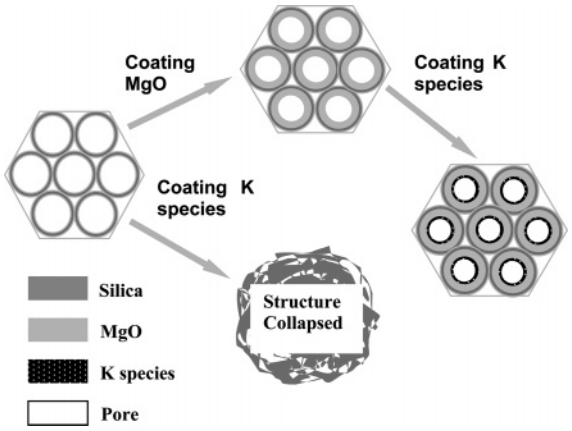

does not change the MgO content of the MS sample. However, the detected ratio of Si/Mg is about 2.0, a bit lower than the expected bulk ratio (2.6). Compared with the data of XPS analysis (Si/Mg ratio of 4.9),[30] it appears that the distribution of MgO is not fully homogeneous in SBA-15, though no MgO crystalline phase emerged in the wide-angle XRD patterns.[36] EDX analysis also shows the existence of potassium species in the activated 26KMS(20) sample (Figure 3B). Nevertheless, the potassium content detected by EDX is lower than that by the ICP method, probably due to the solution of some potassium in the ethanol during the dispersion of the activated 26KMS(20) sample into ethanol needed for TEM measurement. Hence, the information from EDX is beneficial for determining the existence of potassium species existing in the 26KMS(20) sample but not enough for quantitative analysis of the potassium content.

Existence of MgO layer on the surface of SBA-15 obstructs the contact and interaction of potassium species with the siliceous framework, preventing the silica skeleton from the corrosion of alkali metal oxide. As a comparison, directly loading KNO_3 on SBA-15 destroyed the mesostructure after the sample was activated at 873 K. Figure 1d demonstrates the disappearance of three main X-ray diffraction peaks on the 26KS sample, further confirming the crucial role of the MgO layer precoated on the surface of SBA-15 to protect the mesoporous structure. Existence of MgO layer precoated on SBA-15, like the skin wrapping the bone and muscle, prevents the interaction between potassium guest and the siliceous host (Scheme 1).

Figure 4 illustrates the N_2 adsorption−desorption isotherm of the 26KMS(20) sample at 77 K. It is type IV with a clear H1 type hysteresis loop at high relative pressure, quite similar to that of parent SBA-15 (Figure 4a). Nonetheless, an inconspicuous tail exists in the hysteresis of N_2 physisorption curves for the 26KMS(20) sample, and its pore diameter, 6.3 nm, is obviously smaller than that of SBA-15 (8.8 nm, Table 1). This phenomenon originates from the dispersion of potassium species on the surface of the MgO-coated SBA-15 since these guests that dispersed inside the channel of

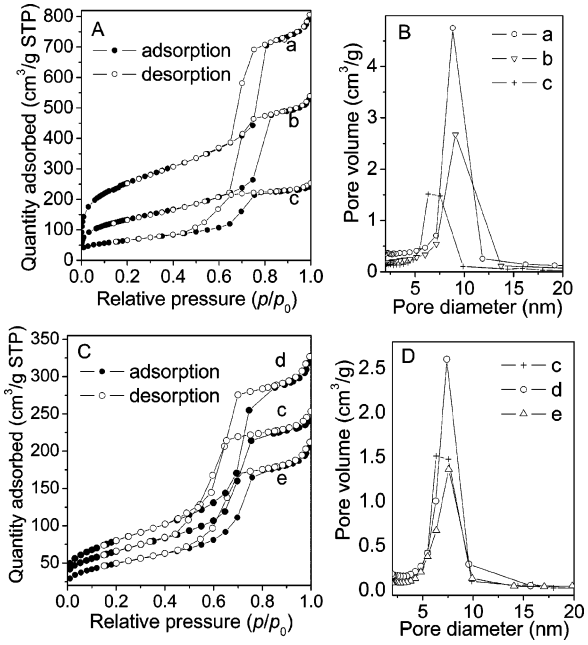

Figure 4. N_2 adsorption−desorption isotherms (A and C) and pore-size distribution (B and D) of (a) SBA-15, (b) MS(20), (c) 26KMS(20), (d) 26KMS(10), and (e) 26KMS(5) samples.

Table 1. Textural Properties and Basicity of the Modified SBA-15 Samples

sample	S_{BET} (m^2/g)	V_p (cm^3/g)	D_p (nm)	basic strength (H–)	ion density of Mg^{2+} (Mg^{2+}/nm^2)	ion density of K^+ (K^+/nm^2)
SBA-15	902	1.25	8.8	<9.3		
MS(20)	481	0.83	9.1	22.5		
26KMS(20)	223	0.39	6.3	27.0	6.3	6.9
26KMS(10)	274	0.51	7.4	27.0	2.4	5.7
26KMS(5)	167	0.33	7.6	<26.5	1.2	9.3

supports will always enhance the roughness of the pore surfaces and then make the pore size of the samples much smaller than that of the supports.[37] In addition, the inflection positions slightly shift toward the lower p/p_0 values and the overall amounts of N_2 adsorption decrease, resulting from the loading of guests in SBA-15.[38] Prior to loading KNO_3, however, the main pore size of the MS(y) supports, which were prepared by one-pot synthesis, was not obviously reduced in comparison with that of SBA-15 though their pore volume decreased as the MgO contents increased;[30] one of the causes for such phenomena is possibly the formation of a comparatively smooth MgO layer in SBA-15.[39] Nonetheless, the pore size distribution of MS is widened more than that of SBA-15 and the adsorption amounts are also decreased, which implied some of the primary pore is obstructed by MgO though the main pore size of MS is not reduced.

The state of magnesium species coated on SBA-15 is important because it directly affects the dispersion of multicoated potassium. It appears that most of the magnesium species are decorated on the surface of SBA-15 to form MgO

(36) Maxim, N.; Magusin, P. C. M. M.; Kooyman, P. J.; van Wolput, J. H. M. C.; van Santen, R. A.; Abbenhuis, H. C. L. *Chem. Mater.* **2001**, *13*, 2958.

(37) Wang, Y. M.; Wu, Z. Y.; Shi, L. Y.; Zhu, J. H. *Adv. Mater.* **2005**, *17*, 323.

(38) Luan, Z. H.; Hartmann, M.; Zhao, D. Y.; Zhou, W. Z.; Kevan, L. *Chem. Mater.* **1999**, *11*, 1621.

(39) Wang, Y. M.; Wu, Z. Y.; Wei, Y. L.; Zhu, J. H. *Microporous Mesoporous Mater.* **2005**, *84*, 127.

because MS samples show similar basic properties such as that of MgO and their total basicities are enhanced with an increase in the MgO contents.[30] However, some of the magnesium species are apt to interact with silanol groups to form a Si−O−Mg layer.[39] These species have not interacted with the template micelles in the initial hydrothermal step but interact with silanol groups during the evaporation and/or calcination process: $Si-(OH)_2 + Mg^{2+} + O^{2-} \rightarrow Si-O_2\cdots Mg + H_2O$ and/or $2Si-OH + Mg^{2+} + O^{2-} \rightarrow Si-O\cdots Mg\cdots O-Si + H_2O$. Most of the magnesium species convert to the smooth MgO*x* layer in calcination, decreasing both the surface area and pore volume of SBA-15 but increasing the intensity of reflection (100) in some cases.[39] Further, part of the magnesium species introduced in SBA-15 may exist in the form of hydroxide because MgO can adsorb moisture in the atmosphere. Wide-angle XRD patterns of MgO stored in the atmosphere reveal the existence of crystalline phase of magnesium hydroxide.[40] In addition, interactions between inorganic salts and PEO-based templates are important factors in the synthesis of block copolymer templated mesoporous oxides.[41−43] Adding magnesium in the synthetic system will affect the structure of SBA-15 and cations undergo complexation with the EO groups of P123 upon evaporation to produce $[M(EO)_x]X_n$ complex.[39] There are connecting micropores and small mesopores between the walls of large-pore channels of SBA-15.[44,45] It is possible for some MgO species to enter the micropores of SBA-15 owing to the curvature and the optical interaction provided by these small pores.[46] So some micropores of SBA-15 are occupied by the magnesium species during the evaporation and calcination process. Although incorporation of MgO may block some mesopores of SBA-15 to form micropores at the same time, the microporosity of MS samples is reduced as the MgO content increases. N_2 adsorption−desorption results proved the hypothesis; the micropore volume is 0.064 cm^3/g for SBA-15 and 0.028, 0.023, 0.018, and 0.006 cm^3/g for MS(5), MS(10), MS(20), and MS(30) samples, respectively. It is clear that micropore volumes of MS samples are lower than that of SBA-15, and about 56, 64, 75, and 90% of the micropore were reduced when MgO was introduced into SBA-15 with contents varying from 5 to 30 wt %.

Table 1 lists the impact of multicoating on the BET specific surface areas and mesopore parameters of SBA-15 that are based on BJH plots, which gives additional proof to the existence of the mesostructure in SBA-15 host even though it has been coated with such large amounts of guests. The 26KMS(20) composite possesses a surface area of 223 m^2/g and pore volume of 0.39 cm^3/g along with the pore size of 6.3 nm. Compared with SBA-15, MS samples show

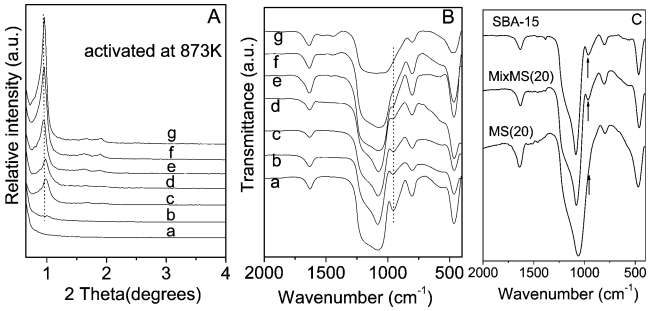

Figure 5. (A) XRD patterns of 26 wt % KNO_3 multicoated MgO/SBA-15 samples with different MgO contents activated in N_2 at 873 K. (B) IR results of different amounts of MgO-coated SBA-15 samples: (a) SBA-15, (b) MS(1), (c) MS(2), (d) MS(3), (e) MS(5), (f) MS(10), and (g) MS(20). (C) IR results of the mixture of SBA-15 with 20 wt % MgO.

relatively low surface area, decreasing from 902 to 320 m^2/g as the MgO content increased from 0 to 30 wt %.[30] When 26 wt % KNO_3 was multicoated on MS samples, the surface areas of resulting 26KMS samples further decreased because the proportion of SBA-15 declined in the resulting samples and the modified KNO_3 occupied the interspaces of the porous hosts. Meanwhile, the decrease in the symmetry of mesostructure for 26KMS(5) also caused the relatively low surface area. Nevertheless, the surface area of 26KMS still exceeds those of the superbasic materials derived from KNO_3 loaded on zeolite KL,[10] Al_2O_3,[26] or ZrO_2.[27] Rather, existence of the ordered mesoporous pore in this composite, as aforementioned, can offer a new candidate for selective adsorption and catalysis.

(B) Protection of MgO on the Mesoporous Structure of SBA-15. To understand the impact of coating MgO on the structure of SBA-15, the textural properties of multicoated 26KMS(*y*) samples with different MgO contents are detected by XRD and N_2 adsorption−desorption experiments. Figure 5 shows the XRD patterns of 26KMS(*y*) samples activated in N_2 at 873 K. As the content of MgO increased from 1 to 20 wt %, the order of the remaining mesostructure of SBA-15 was enhanced. When no MgO was precoated to form a protection layer, the mesoporous structure of bare SBA-15 would be entirely destroyed by the strong basic potassium species formed in the decomposition of KNO_3 guest at high temperature. Likewise, introducing 1 wt % MgO still failed to protect siliceous host and the mesostructure of SBA-15 rarely remained. As the amount of MgO in situ coated on SBA-15 rose to 2 wt %, the main peak of the hexagonal lattice emerged in the low-angle XRD patterns as shown in Figure 5A. An increase in the amount of the in situ coated MgO significantly improved the protection of the order of SBA-15 after the host was loaded with 26 wt % KNO_3 and activated at 873 K, and the *p*6*mm* symmetry of SBA-15 was almost completely preserved when the in situ coated MgO content achieved 10 wt %. Actually, the coated MgO consumes the silanol groups of SBA-15 to form the passivation layer, preventing the basic potassium guests from corroding the mesostructure of SBA-15. Figure 5B illustrates the FT-IR transmission spectra of MS(*y*) samples with different MgO contents. The Si−O−Si bending band at around 960 cm^{-1} in the spectrum was assigned to silanol groups in mesoporous SBA-15,[47] and its relative intensity gradually weakened with the increased amount of MgO. The

(40) Sun, L. B.; Wu, Z. Y.; Kou J. H.; Chun, Y.; Wang, Y.; Zhu, J. H.; Zou, Z. G. *Chin. J. Catal.* **2006**, in press.
(41) Soler-Illia, G. J. de A. A.; Crepaldi, E. L.; Grosso, D.; Sanchez, C. *Curr. Opin. Colloid Interface Sci.* **2003**, *8*, 109.
(42) Sanchez, C.; Soler-Illia, G. J. de A. A.; Ribot, F.; Lalot T.; Mayer, C. R.; Cabuil, V. *Chem. Mater.* **2001**, *13*, 3061.
(43) Soler-Illia, G. J. de A. A.; Sanchez, C. *New J. Chem.* **2002**, *24*, 493.
(44) Ryoo, R.; Joo, S. H.; Kruk, M.; Jaroniec, M. *Adv. Mater.* **2001**, *13*, 677.
(45) Joo, S. H.; Ryoo, R.; Kruk, M.; Jaroniec, M. *J. Phys. Chem. B* **2002**, *106*, 4640.
(46) Tian, B. Zh.; Liu, X. Y.; Yu, Ch. Zh.; Gao, F.; Luo, Q.; Xie, S. H.; Tu, B.; Zhao, D. Y. *Chem. Commun.* **2002**, 1186.

960 cm^{-1} band degenerated to the shoulder of the 1080 cm^{-1} band in the MS(5) sample, whereas the amount of the in situ coated MgO reached 10 wt %; the band near 960 cm^{-1} was almost invisible. Coating the 20 wt % MgO on SBA-15 made the band around 960 cm^{-1} entirely vanish as demonstrated in Figure 5B. To avoid the possibility that disappearance of the 960 cm^{-1} band in the spectrum of MS-(20) is due to the sample being too concentrated in the pellet so that the Si−O−Si bands look "square", the ratio of KBr/MS(20) was adjusted to reduce the concentration of the sample for FT-IR experiments. The same result was obtained: the 960 cm^{-1} band clearly disappeared in the MS-(20) sample (Figure 5C). However, if 20 wt % MgO was mechanically mixed with SBA-15, it could not cause the disappearance of the 960 cm^{-1} band in the IR spectrum of SBA-15; contrarily, the three bands around 960, 800, and 465 cm^{-1} of SBA-15 still kept their original positions as demonstrated in Figure 5C. The same experiments were performed in the samples of ZnO-modified SBA-15 and similar phenomena were observed.[47] Based on the FT-IR experiments together with the previous XRD results, it is very likely that the mesostructre of 26KMS(*y*) samples can be perfectly preserved after thermal activation as long as the SBA-15 is in situ coated with the 10 wt % MgO or more in the one-pot synthesis procedure. Rather, it is reasonable to say that MgO can form a compact passivation layer on the surface of SBA-15 provided the amount of coated MgO exceeds 10 wt %. Assuming the number of silanol groups in SBA-15[48] is nOH $\approx$ 3.7 /nm^2 and the BET surface area of SBA-15 is around 900 m^2/g, theoretically it needs about 10 wt % MgO to completely consume the silanol groups of the host in case magnesium species react with silanols according to stoichiometry. This result is in good agreement with the IR results where almost no Si−OH bending bands are observed around 960 cm^{-1} on the spectrum of MS(10). Raman results of MS(*y*) samples give further evidence on the consuming of silanol groups of SBA-15 by MgO. Raman spectra of porous silica in the O−H stretching range (3000−3800 cm^{-1}) display a broad band arising from the contribution of different hydrogen-bonding interacting hydroxyl species, and a narrow band at 3750 cm^{-1} relates to the O−H stretching in isolated silanols.[49] As seen in Figure 6, the narrow Raman band at 3750 cm^{-1} in SBA-15 is higher than that in MS(3) composite, and it is almost invisible in the sample of MS(10). Due to the weak Raman signal of siliceous materials and the fluorescence effect of magnesium species, it is impossible to get the Raman spectrum of the MS(20) sample. On the other hand, N_2-physisoption experiments revealed that 26KMS(10) possessed the highest pore size distribution among 26KMS(*y*) samples (Figure 4D); its surface area and pore volume, 274 m^2/g and 0.51 cm^3/g, respectively, are larger than that of 26KMS(5) and 26KMS-(20) samples (Table 1). Referring to these results, the 10 wt % MgO seems to be the optimal choice for the formation of a protection layer on SBA-15. Nonetheless, it is worthy to point out that even though the mesoporous host is in situ coated with 5 wt %MgO, the resulting 26KMS(5) sample still displays a good texture with the surface area of 167 m^2/g and pore volume of 0.33 cm^3/g, respectively.

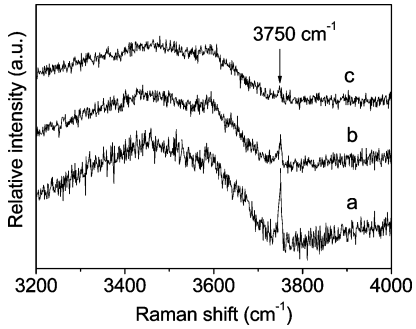

Figure 6. Raman spectra of (a) SBA-15, (b) MS(3), and (c) MS(10).

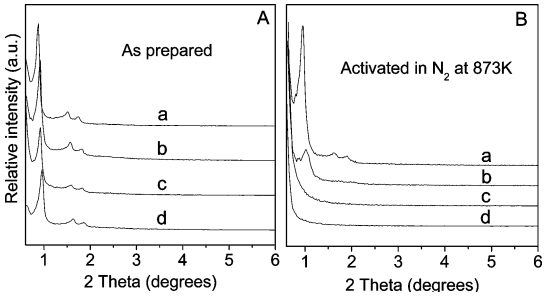

Figure 7. XRD patterns of multicoated SBA-15 samples that were precoated with alkaline-earth metal oxides and then loaded with 26 wt % KNO_3, before (A) and after (B) activation in N_2 at 873 K. (a) MgO/SBA-15(5), (b) CaO/SBA-15(7), (c) SrO/SBA-15(13), and (d) BaO/SBA-15(20).

Other alkaline-earth metal oxides such as CaO, SrO, and BaO were also in situ coated on SBA-15 through one-pot synthesis to examine whether they have properties such as MgO to protect the mesostructure of the siliceous host. CaO/SBA-15(7), SrO/SBA-15(13), and BaO/SBA-15(20) are synthesized with the same oxide molar composition as that of the MS(5) sample, and Figure 7A shows their XRD patterns after the samples were loaded with 26 wt % KNO_3. Before thermal activation at 873 K, all samples give the well-resolved XRD patterns such as that of SBA-15, indicating the existence of hexagonal pore structure in the composites. Wide-angle XRD patterns of these samples revealed that the in situ coated oxide, say, 7 wt % CaO, 13 wt % SrO, or 20 wt % BaO, can be well-dispersed on the SBA-15 support. And these guests also consume the silanol groups of SBA-15 like what the MgO did (Supporting Information, SI 1). However, after activation at 873 K among them only the sample 26KNO_3/CaO/SBA-15(7) maintained one main peak in the XRD pattern like 26KMS(5), but the relative intensity is rather low and the other two weak peaks related to crystal lattice (110) and (200) disappear, mirroring the weaker ability of calcium oxide to protect the mesostructure of SBA-15 than MgO. Other two alkaline-earth metal oxides, SrO and BaO, do not have the protective function of SBA-15 at all as shown in Figure 7B. It is still in doubt why the other alkaline-earth metal oxides such as CaO, SrO, and BaO cannot play the same roles as that of MgO to interdict the

(47) Jiang, Q.; Wu, Z. Y.; Wang, Y. M.; Cao, Y.; Zhou, C. F.; Zhu, J. H. *J. Mater. Chem.* **2006**, *16*, 1536.
(48) Shenderovich, I. G.; Buntkowsky, G.; Schreiber, A.; Gedat, E.; Sharif, S.; Albrecht, J.; Golubev, N. S.; Findenegg, G. H.; Limbach, H.-H. *J. Phys. Chem. B* **2003**, *107*, 11924
(49) (a) Anedda, A.; Carbonaroa, C. M.; Clementea, F.; Cordab, L.; Corpinoa, R.; Ricci, P. C. *Mater. Sci. Eng. C* **2003**, *23*, 1069. (b) Anedda, A.; Carbonaro, C. M.; Clemente, F.; Corpino, R.; Ricci, P. C. *J. Phys. Chem. B* **2003**, *107*, 13661.

interaction between the siliceous host and the strong basic potassium guest; further study is desirable.

Some common metal oxides such as ZnO, ZrO_2, and Al_2O_3 were also introduced into SBA-15 through the one-pot synthesis procedure with the same mass percentage of 20%. Aluminum and zirconium can easily be incorporated into the silica skeleton of SBA-15.[38,50] ZnO is widely used in photoluminescence science[51] but seldom serves in solid base materials. Thus, their properties may differ from MgO's. As seen in the Supporting Information, SI 2, the mesoporous structure of the in situ coated SBA-15 can be partially reserved when loaded with 26 wt % KNO_3 and activated at 873 K; however, the intensities of the XRD patterns obviously decreased. Clearly in these cases, more ordering of the mesostructure in the hosts is lost. IR spectra revealed that coating of ZnO or ZrO_2 of 20 wt % expended thoroughly the silanol groups of SBA-15 while the moiety silanol groups of the host was consumed by loading Al_2O_3 (Supporting Information, SI 2). However, these oxides cannot effectively protect the mesoporous structure of SBA-15; similarly, ZnO failed to protect amorphous silica against the corrosion of caustic soda.[52] All three metal oxides possess amphoteric features more or less, which may induce the failure in interdicting the corrosion of basic potassium species because the protector itself can react with them.

Table 1 lists the basic strength of the potassium-containing mesoporous composite. In the titration with Hammett indicators, both 26KMS(10) and 26KMS(20) samples can change the acidic, colorless form of 4-chloroaniline ($pK_a = 26.5$) and aniline ($pK_a = 27.0$) to their basic color (pink and violet red), which can be assigned as a characteristic of superbasic material according to Tanabe's definition.[53] And this is the first evidence of superbasic property on the mesoporous silica modified with neutral potassium salt such as KNO_3. CO_2-TPD results confirm the unusual strong basicity of KMS composites. As is evident from Figure 1B, SBA-15 has a weak ability to adsorb CO_2; therefore, only a little desorption occurs round 350 K in the CO_2-TPD spectrum. In situ coating of MgO on SBA-15 enables the porous silica to own a considerable basicity so that substantial CO_2 desorption emerges with the climax at 373 K (Figure 1B, curve b). Moreover, this desorption of CO_2 on the MgO-coated sample remains until 600 K to form a continuous tail, and the amount of the desorbed CO_2 dramatically increases from 0.04 to 0.73 mmol/g. Loading KNO_3 on the MgO-coated SBA-15 followed by activation at 873 K leads to the appearance of new CO_2 desorption around 873 K on the *x*KMS(20) samples with the variety of loading amount of KNO_3 as shown in Figure 1B, while the first desorption of CO_2 in the spectrum shifts from 373 to 418 K, indicating the close relation between the dramatic increase of basicity and the incorporation of potassium species. In the case of loading the 20 wt % KNO_3, the resulting absolute desorption of CO_2 (0.79 mmol/g) is not changed too much in comparison with that of the MgO-coated support (0.73 mmol/g), but the desorption temperature is significantly different; one-fifth desorbs at 873 K while the rest desorbs around 420 K. As the loading amount of potassium salt increases to 26 wt %, the total amount of CO_2 desorption increases one-fourth and more CO_2 desorbs at 420 K while the CO_2 desorption at 873 K remains constant. Further increase in loading amount of KNO_3 is not beneficial for creating strong basic sites on the modified SBA-15, and the total amount of CO_2 desorbed from the sample of 35KMS(20) decreases about one-tenth while the amount of CO_2 desorbed at 873 K declines from 0.16 to 0.12 mmol/g.

Siliceous SBA-15 exhibits a very weak basicity and its basic strength (H_-) is below 9.3. Coating MgO on SBA-15 through one-pot synthesis or impregnation can improve the basic strength (H_-) to 22.5,[30,54] but fail to produce the superbasic sites. It is clear that dispersion of potassium species in the modified mesoporous SBA-15, probably in the form of nanoparticles, results in the superbasic sites with basic strength (H_-) above 26.5. Here the suitable MgO protection layer on SBA-15 plays a vital role because it should strictly wrap the mesoporous siliceous host to avoid the corrosion of potassium oxides on the silica; otherwise, the multicoated composite will lose the valuable mesostructure. For this propose the candidate should be easily dispersed on the silica owing to the strong host−guest interaction, instead of aggregation or crystallization of the guests themselves. Mg^{2+}, Zn^{2+}, Fe^{3+}, and Zr^{4+} are known to more aptly react with surface silanol groups of SBA-15 and thus the high dispersion of relevant oxide species can be achieved after calcination, while Cu^{2+}, Ni^{2+}, and Cr^{3+} tend to condense to M−O−M and then oxide clusters during calcination.[37,39] In contrast, anions have a minor impact on the dispersion of precursor salt and the conversion to oxide.[55] Two magnesium salts, chloride and acetate, were used to coat SBA-15 through one-pot synthesis for dispersing KNO_3 and successfully realized the generation of superbasicity on the mesoporous silica. One may doubt whether the precoating MgO on SBA-15 is limited to direct synthesis method, and our experiments exclude this suspicion. Superbasic sites can also be generated on the *x*KMS(20) samples where MgO is pre-decorated on SBA-15 by impregnation method. However, it should point out that both the surface area and the pore volume of the MS(20) prepared by impregnation are lower than those prepared by direct synthesis,[30] which may have an impact on the potential application of the resulting mesoporous strong bases.

(C) Dispersion and Decomposition of KNO_3 on the MgO-Modified SBA-15. The dispersion of KNO_3 on the MgO-modified SBA-15 was displayed in Supporting Information, SI 3. Considering the textural properties and surface Mg^{2+} ion density of SBA-15, MS(20) is chosen to support potassium salt for further research because the BET surface area and pore volume of MS(30) are much smaller while the surface ion density of MS(10) is somewhat lower.[30] No

(50) Newalkar, B. L.; Olanrewaju, J.; Komarneni, S. *J. Phys. Chem. B* **2001**, *105*, 8356.
(51) Chen, J.; Feng, Z. C.; Ying, P. L.; Li, M. J.; Han, B.; Li, C. *Phys. Chem. Chem. Phys.* **2004**, *6*, 4473.
(52) Jiang, Q.; Xu, J. H.; Cao, Y.; Liu, L.; Zhu,J. H. *Stud. Surf. Sci. Catal.* **2005**, *158*, 1749.
(53) Tanabe, K. In *Catalysis by acids and bases*; Imelik, B., Nacceche, C., Condurier, G., Ben Taarit, Y., Vedrine, J. C., Eds.; Elesvier: Amsterdam, 1985; p 1.
(54) Wei, Y. L.; Cao, Y.; Zhu, J. H. *Stud. Surf. Sci. Catal.* **2004**, *154*, 878.
(55) Wu, Z. Y.; Wei, Y. L.; Wang, Y. M.; Zhu, J. H. *Chin. Sci. Bull.* **2004**, *49*, 1332.

Table 2. Ion Content of Potassium in KNO_3-Loaded SBA-15 Samples

	K^+ content (%)	
sample	as prepared	activated at 873 K
26KS	10.2	9.7
26KMS(20)	9.8	10.5

characteristic peak of KNO_3 was found on the XRD patterns of 10KMS(20), indicating the good dispersion of the potassium salt. When the amount of KNO_3 increased to 16 wt %, characteristic peaks of KNO_3 emerged on the XRD patterns of 16KMS(20) sample with the 2θ value of 23.6, 29.4, and 33.8°, respectively, revealing the existence of residual phase of KNO_3 remained. As the amount of KNO_3 guest exceeded 20 wt %, another two XRD peaks appeared on the patterns of *x*KMS(20) samples with the 2θ value of 27.2 and 39.4°, and their intensity increased as the amount of KNO_3 rose, implying the formation of another phase of KNO_3 in these composites (JCPDS 76-1693). As a comparison, KNO_3 was loaded on bare SBA-15 and Supporting Information, SI 3B showed the XRD patterns. Through the comparison of the XRD patterns of 26KMS(20) and 26KS samples before and after activation, it is clear that coating MgO on SBA-15 does not obviously promote the dispersion of KNO_3 at room temperature, but accelerates the dispersion and/or decomposition of the precursor at high temperature because the residual KNO_3 disappeared in the former sample but persisted on the latter after 873 K activation. As is evident from Supporting Information, SI 3B, the characteristic peaks of KNO_3 completely disappear on the patterns of *x*KMS(20) after activation at 873 K, even though the loading amount of KNO_3 is raised to 35 wt %, which further implies the interaction between KNO_3 and magnesium species and such interaction seems to accelerate dispersion and/or decomposition of KNO_3. It is in doubt that potassium sublimation occurs during activation at 873 K to cause the disappearance of KNO_3 residual phase. However, ICP analysis in Table 2 excludes this suspicion. The ion content of potassium of both 26KMS(20) and 26KS samples remained unchanged within the experimental error.

Figure 8 depicts the decomposition of KNO_3 on the MgO-modified SBA-15 in temperature-programmed decomposition (TPDE) process. The possible decomposition mechanism of KNO_3 has been discussed in previously reported papers.[26,28,32,56] In general, thermal decomposition of KNO_3 consists of two steps: it first converts to nitrite and then second decomposes to potassium oxide and nitrogen oxides. The K_2O derived from KNO_3 support is estimated as the main basic species. Gaseous products O_2, NO, NO_2, and other nitrogen oxides could be detected during the decomposition of KNO_3. Consequently, the detected nitrogen oxides in the experiment represent the amount of KNO_3 decomposed. A majority of NO*x* is detected at 873 K whether or not the porous sample has been in situ coated with MgO. However, the value of climax is different; the former is significantly larger than the latter. Additionally, about two-thirds of NO*x* releases from 26KS after the sample is held at 873 K for 2 h, and based on the profile shape of NO*x* emission, the

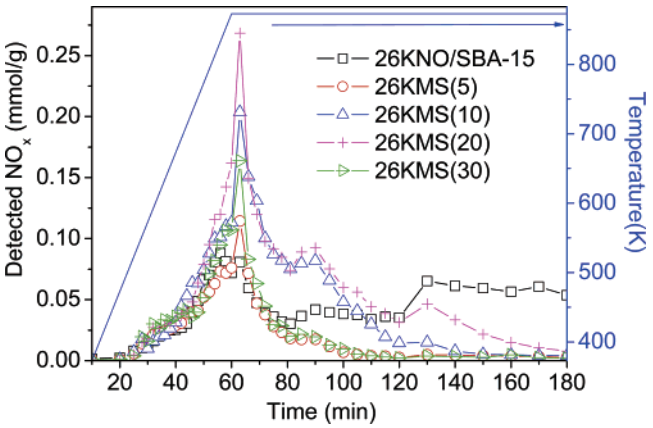

Figure 8. Temperature-programmed decomposition of KNO_3 on the MgO-modified SBA-15 samples.

decomposition of KNO_3 on 26KS seems unfinished, whereas most of the NO*x* emits within the first hour on the MgO-modified SBA-15 samples. These results indicate that the existence of MgO in SBA-15 promotes the decomposition of KNO_3.

IR spectra of 26KMS(*y*) samples before and after activation at 873 K were measured to examine the decomposition of KNO_3 guests decorated on SBA-15 and MS samples (see Supporting Information, SI 4). All as-prepared samples are characterized with 1390 and 1764 cm^{-1} bands of nitrate. Activation at 873 K only slightly reduces the intensity of 1390 cm^{-1} band of 26KS sample; meanwhile, the 1764 cm^{-1} insists on the spectrum, mirroring the existence of residual KNO_3 in the sample as revealed by the TPDE result aforementioned. Contrarily, both 1390 and 1764 cm^{-1} bands disappear on 26KMS(5) sample after activation at 873 K, indicating the decomposition of KNO_3 guest. For those 26KMS(*y*) samples coated with more MgO, 1497 and 1413 cm^{-1} characteristic bands of carbonate emerge due to the contamination of basic sites by the CO_2 in the atmosphere. Based on these phenomena, the promotion of MgO coated on SBA-15 on the decomposition of KNO_3 is approved.

Apparently, the protection layer on SBA-15 should be beneficial for the decomposition of potassium precursor to form strong basic sites. KNO_3 usually decomposes above 873 K,[32] and its decomposition temperature can be dramatically lowered when it is highly dispersed on the weak acidic or amphoteric supports.[28,32,57] The interaction between the acidic sites of support with the newly formed basic species can accelerate the decomposition of precursor salt, but decrease the final basicity of the composite so that it is better to disperse and decompose the potassium precursor salt on a basic support like MgO. However, the actual interaction between KNO_3 and MgO at high temperature is unknown, which spurs us to load KNO_3 directly on MgO itself. After activation at 873 K for 2 h, the sample of 26 wt % KNO_3/MgO exhibits the base strength (H_-) of 27.0, which implies that KNO_3 can be decomposed near 873 K in the case of the loading on MgO, and then form superbasic sites. A similar process will be realized on the layer of MgO over the mesoporous silica that protects the siliceous framework

(56) Zhu, J. H.; Wang, Y.; Yamaguchi, T. *Chin. J. Catal.* **1996**, *17*, 286.

(57) Wang, Y.; Zhu, J. H.; Huang, W. Y. *Phys. Chem. Chem. Phys.* **2001**, *3*, 253.

and supports the guests of potassium guest, which is the crucial function of the precoated MgO in the formation of mesoporous superbasic material. The MgO should be well-dispersed to cover the surface of the siliceous SBA-15 support so that the corrosion of potassium species is interdicted and the mesoporous structure of the host remains. At the same time, the dispersed MgO should form a suitable microenvironment for the potassium precursor salt to form basic potassium species, leading to unusual strong basicity. Here the amount of the MgO coated on SBA-15 directly affects the final basicity of the resulting solid base.

As mentioned earlier, the 26KMS(5) sample displayed mesoporous texture properties after activation at 873 K; however, its basic strength is not as strong as that of the 26KMS(10) and 26KMS(20) samples. 26KMS(5) sample failed to change the indicator of $pK_a = 26.5$ to their basic color in titration with the Hammett indicator, which indicates the lack of superbasic sites on this composite and one of the reasons is the insufficient precoated MgO. The atomic ratio of potassium to magnesium in the sample of 26KMS(5) is 2.77; therefore, the number of potassium atoms exceeds that of magnesium. Besides, coating of 5 wt % MgO could not entirely consume the silanol groups of SBA-15 as aforementioned. It is easy to imagine that the excrescent potassium species will react with the bare surface of the siliceous host to form the compounds with lower basic strength as that revealed in the zeolite-supported KNO_3.[9,29] Increasing the amount of MgO coated on SBA-15 to 10 wt % changes the atomic ratio of K/Mg to 1.41, which causes the appearance of superbasic sites in the sample but the amount of soluble base remained unchanged (0.68 mmol of OH^-/g). When the amount of MgO precoated achieves 20 wt %, the K/Mg ratio reaches 0.70 and the surface density of two cations in this sample is much closer. As a result, 26KMS(20) composite possesses the largest CO_2 desorption among the samples tested in the CO_2-TPD experiment as demonstrated in Figure 1B. Coating SBA-15 with 30 wt % MgO does not cause an obvious difference in resulting basicity; both the maximum basic strength ($H_- = 27.0$) and the soluble basicity (1.04 mmol of OH^-/g) are the same as those of 26KMS(20).

The loading amount of KNO_3 also impacts the final basicity of the resulting sample. Among the *x*KMS(20) samples with the *x* value varying from 10 to 35, only 10KMS(20) cannot change the indicator of $pK_a = 26.5$ to its basic color, while other *x*KMS(20) samples exhibit superbasicity once the mass percentage of KNO_3 exceeds 16 wt %. That is to say, the amount of KNO_3 loaded on MS(20) support should exceed the spontaneous dispersion threshold in order to generate the unusually strong basic sites. The same situation has been reported in the case of Al_2O_3 and ZrO_2, where a kind of overlapped structure of basic potassium species is believed to relate to the unusual strong basicity.[28,32] Otherwise, no superbasic site is detected in the resulting sample like 10KMS(20), though the precursor salt is well-dispersed and decomposed. Further investigation is thus requested for a deep understanding of these phenomena.

Conclusion

1. New basic porous silica with mesoporous structure and strong basicity is prepared by using the multicoating method. Siliceous SBA-15 is wrapped by MgO at first to prevent the etching of basic potassium species, and then neutral salt KNO_3 is dispersed and decomposed on the layer of MgO to form the strong basic sites with the strength of $H_- = 27.0$.

2. Magnesium species have the proper ability to consume silanol groups of SBA-15 when they are introduced into SBA-15 and transformed to MgO. As a result, 10 wt % MgO can almost completely consume the silanol groups of SBA-15 and 26KMS(10) sample shows the best textural properties.

3. Other alkaline-earth metal oxides and some amphoteric metal oxides are decorated in SBA-15, and some of them can consume silanol groups of SBA-15 but they fail to form a compact passivation layer like MgO.

4. Loading 16−35 wt % KNO_3 on the MS(20) sample leads to the formation of superbasic sites provided the activation is at 873 K.

Acknowledgment. We would like to thank NSF of China (20273031 and 20373024) and Analysis Center of Nanjing University for financially supporting this research. Dr. Kai Shen from Nanjing University of Aeronautics and Astronautics is acknowledged for the fulfillment of TEM experiments.

Supporting Information Available: XRD and IR spectra of various samples. This material is available free of charge via the Internet at http://pubs.acs.org.

CM0608138